Highly Effective Sulfated Zirconia Nanocatalysts Grown out of Colloidal Silica at High Temperature

Guangshan Zhu,[a] Ce Wang,*[a] Yahong Zhang,[a] Na Guo,[a] Yiyang Zhao,[a] Runwei Wang,[a] Shilun Qiu,[a] Yen Wei,[b] and Ray H. Baughman[c]

Abstract: A large surface-to-volume ratio is a prerequisite for highly effective catalysts. Making catalysts in the form of nanoparticles provides a good way to achieve the aim. However, agglomeration of nanoparticles during the preparation and utilization of nanocatalysts remains a formidable problem. Here, we present a novel approach in which nano units of catalysts are formed in the matrix of a colloidal carrier, with assistance of a cross-linking agent, and then grow out of the carrier upon calcination at high temperature. This ensures that the catalysts not only do not agglomerate, but also have a low cost and high catalytic efficiency due to the large surface-to-volume ratio and the absence of carbon deposition. The technique is demonstrated by the successful preparation of a binary nanocatalyst that consists of a silica nanoparticle core and a sulfated zirconia (SZ) nanocrystal shell (JML-1). The synthesis was achieved by converting sulfated zirconia (SZ) and silica solutions into a composite gel by means of sol–gel processing in the presence of triethoxysilane as the cross-linking agent, followed by heating at 50 °C and calcining at 550 °C. Relative to other catalysts, such as pure SZ, non-nanodispersed SZ over silica (SZ/SiO_2), and zeolites Y, Beta, and ZSM-5, JML-1 exhibits superior catalytic activity in many reactions. For example, the activity of JML-1 in the production of gasoline by alkylation of 1-butene with isobutene remained at 95 % or higher after 20 h of reaction and was over 90 % after being regenerated five times. In sharp contrast, SZ and SZ/SiO_2 give a high activity only for 2 h and the initial activity of zeolites Beta and ZSM-5 are about 88 and 60 %, respectively. These findings demonstrate that non-agglomerated nanoparticles anchored onto a carrier surface can be prepared and the technique provides a versatile route to new highly effective nanocatalyst systems.

Keywords: heterogeneous catalysis · nanostructures · sol–gel processes · sulfur · zirconium

Introduction

Catalytic materials are widely used in industrial chemical processes. However, challenges remain to maximize their efficiency, to keep their stability and activity over a long operating period, and to achieve re-usability by regeneration for cost-reduction and environmental considerations.[1] Sulfation-modified metal oxides, such as sulfated zirconia (SZ), and zeolites are two important solid catalysts that are used in acid-promoted catalytic reactions, such as alkylation, dehydration, isomerization, cracking, and so forth.[2] In particular, they are the candidates for potential replacement of the liquid acid catalysts, such as hydrofluoric acid or sulfuric acid in commercial gasoline refining processes. Modified complex oxides are good candidates because of their strong acidity. However, such oxides in conventional forms are not effective enough, due to the small surface-to-volume ratio and their activity decreases quickly after several hours of reactions.[3] Although the zeolites possess larger surface areas, the deposition of carbon and the formation of coke in and on them limit their industrial applications as catalysts.[4,5] To raise the surface-to-volume ratio, many metal oxide nanoparticle catalysts have been investigated.[6,7] However, in the process of sulfation at high temperatures of over 500 °C, the nanoparticles are agglomerated, leading to a reduction in surface-to-volume ratio. Silica-supported metal oxides, especially SZ over silica (SZ/SiO_2), have attracted particular at-

[a] Dr. G. Zhu, Prof. C. Wang, Y. Zhang, N. Guo, Y. Zhao, R. Wang, S. Qiu
The Jilin University Alan G. MacDiarmid Institute
Jilin University, Changchun, 130023 (China)
Fax: (+86) 431-5168292
E-mail: cwang@jlu.edu.cn

[b] Prof. Y. Wei
Department of Chemistry
Drexel University, Philadelphia, PA 19104 (USA)

[c] Prof. R. H. Baughman
The Nanotechnology Institute
University of Texas at Dallas
Richardson, TX 75083-0688 (USA)

  DOI: 10.1002/chem.200400288

tention since 1988,[8–12] due to their higher thermal stability, bigger surface-to-volume ratio and lower cost than the SZ.

SZ/SiO_2 is usually prepared by a sol–gel process, and its catalytic activity depends on the reactivity of alkoxide precursors, amount of absorbed sulfuric acid, thermal treatment conditions, and the number of active SZ sites on the surface.[13–18] Because of different hydrolysis rates of the ZrO_2 and SiO_2 precursors, a phase separation (colloid agglomeration) occurs during the sol–gel reactions. Consequently after thermal treatment, a SZ nanocatalyst with a large surface-to-volume ratio cannot be obtained, although SZ is able to partly move onto the silica surface during calcination.[19] In addition, the acid strength, as indicated by the concentration of SO_4^{2-}, is not adjustable by the techniques of co-precipitation and impregnation as reported in the literature.[20] It is apparent that the use of silica carrier as described above could not achieve high catalytic efficiency of SZ. Here, we present a novel approach to prepare highly efficient SZ/SiO_2 catalysts with a shell of SZ nanocrystals growing on a core of silica nanoparticles; this catalyst is designated as JML-1 to distinguish it from other binary SZ/SiO_2 composite catalysts.

Experimental Section

Synthetic methods

Synthesis of JML-1: A solution of SiO_2 was obtained by hydrolyzing tetraethoxysilane (TEOS, 31.19 g) in a mixture of THF (21.26 g), H_2O (6.74 g)and HCl (2 M, 5 g) under magnetic stirring at 65–70 °C for 3 h. A solution of sulfated zirconia was prepared by placing ethanol (10 g) and of isobutoxylzirconium ($Zr(OC_4H_9)_4$, 80 wt % in butanol, 10 g) into a flask under magnetic stirring at room temperature, followed by addition of a mixture of ethanol (6.5 g), distilled water (1.5 g) and H_2SO_4 (18 M, 5 g). Alternatively, the SZ solution was obtained by gently stirring a solution of of ethanol (16.5 g), $Zr(OC_4H_9)_4$ (10 g), distilled water (1.5 g) and of vitriol (5 g) in a 500 mL flask until the system became a wet gel, which was mechanically crushed with intensified stirring to afford a transparent solution. The SiO_2 solution was then mixed with the SZ solution at a proper molar ratio, depending on the desired Zr/Si ratio in the final product, under magnetic stirring for 12–24 h. Finally, the cross-linking agent triethoxysilane ($HSi(OC_2H_5)_3$) was added to the system to form a transparent binary gel. The gel was dried at room temperature for 2 days, ground into fine powder and then heated at 50 °C for about 5 h, followed by heating to 550 °C at a rate of 10 °C h^{-1} and calcining at 550 °C for an additional 3 h. The calcined products were stored in a desiccator for use later.

Characterization: The high-resolution TEM images were obtained on a JEOL 2010 electron microscope with an acceleration voltage of 200 kV. Measurement of nitrogen adsorption isotherms was performed on a Micromeritics ASAP 2010 system. Before each measurement, the samples were degassed at 200 °C for 2 h. The pore size distribution was calculated by using the Horvath--Kawazoe (HK) method.

IR spectra of the samples with and without pyridine were recorded on an FT-IR spectrometer (PE 430) with a resolution of 1 cm^{-1}. In order to measure the pyridine adsorption, the samples were pressed into the thin pellets, and placed into a quartz cell with CaF_2 windows. The sample pellets were evacuated at 400 °C for 2 h ($< 10^{-5}$ Torr). After cooling down to room temperature, the pellets were exposed to a pyridine environment (10 Torr) at 25 °C. IR spectra were recorded after adsorption of pyridine for 1 h and evacuation at 150, 250, 350, and 450 °C for 1 h.

NH_3 temperature-programmed desorption (TPD) curves were obtained in a temperature range of 120–600 °C, at a rate of 15 °C min^{-1}. The adsorption of ammonia onto the sample was carried out at 25 °C. Subsequently, the removal of ammonia was performed at 500 or 550 °C for 1 h by purging air or pure nitrogen. Blank runs were carried out under the same conditions, but with no NH_3 adsorbed. The NH_3 TPD curves were obtained after substraction of the blanks run.

Catalytic reactions: The catalytic performance of the samples was evaluated by using GC-8A and GC-17A (Shimazu) instruments equipped with thermal conductivity and flame ionization detectors. The catalytic alkylation of isobutane with 1-butene was investigated at 2 MPa by using a stainless-steel apparatus equipped with a one-through stainless-steel flow reactor. A typical reaction was performed with JML-1 (1 g), isobutene/1-butene (12:1 mol/mol), and weight hourly space velocity (WHSV) of 4 h^{-1} at 25 °C. A typical reaction of the condensation of diethylene glycol to dioxane was carried out in a reactor with diethylene glycol (100 mL) and the catalyst (20 g), only the product in the range 100–103 °C was collected. After being dried with MgSO4, the pure dioxane was finally obtained.

Results and Discussion

In order to anchor SZ nanocrystals onto the surface of silica, the preparation of JML-1 was carried out by a sol–gel process that involved the use of a cross-linking agent, triethoxysilane. Thus, tetraethoxysilane was hydrolyzed in a mixture of THF and water under HCl catalysis to yield the silica solution. Likewise, $Zr(OC_4H_9)_4$ was hydrolyzed in alcohol/water in the presence of vitriol or sulfuric acid (Zr/S = 1:2, mol/mol) leading to the SZ solution. The transparent silica and SZ solutions were then mixed at the desired molar ratios. After stirring at room temperature for 24 h, a certain amount of triethoxysilane was added to effect gelation. The as-obtained binary gel was heated at 50 °C for 5 h followed by calcination at a heating rate of 10 °C h^{-1} up to 550 °C to afford the JML-1 catalyst. The introduction of triethoxysilane accelerates the gelation process to give a rapid formation of the silica network, so that the mobility of ZrO_2 colloidal particles is limited in the network. Such a hindered mobility prevents the ZrO_2 nanoparticles from self-aggregating in the solution state and allows for migration from the core to the surface of condensing silica at high temperature.

At a fixed molar ratio of Zr/Si, the amount of triethoxysilane cross-linking agent was found to have significant effect on the gel time, the size of SZ nanocrystals, and the percentage coverage of SZ on the silica surface, which is directly related to the acidity of the catalysts.[21] As the amount of triethoxysilane was changed from 0.01 to 0.06 to 0.11 mol % based on SiO_2 for JML-1_{40} (Zr/Si = 40:100, mol/mol), the gel time was shortened from 24 h to 0.5 h or less. As shown in Figure 1, the average size of SZ nanocrystals with a hexagonal structure also decreased from 5.5 × 11 nm (A) to 3.3 × 7.2 nm (B), to 3.5 × 5.5 nm (C). The percentage coverage decreased from 92 % (A) to 45 % (B) to 12 % (C). Such a decrease in the SZ coverage with the increase of amount of triethoxysilane would reduce the effective surface area of SZ. This is understandable, because the increase in the amount of cross-linking agent should result in a denser silica network, which would prevent self-aggregation of SZ nanoparticles in the silica matrix; on the other hand, it would hinder the migration of ZrO_2 nanoparticles through the network to the surface. Consequently the percentage coverage of the SZ nanoparticles on the silica surface reduced when the amount of the cross-linking agent was increased. Based

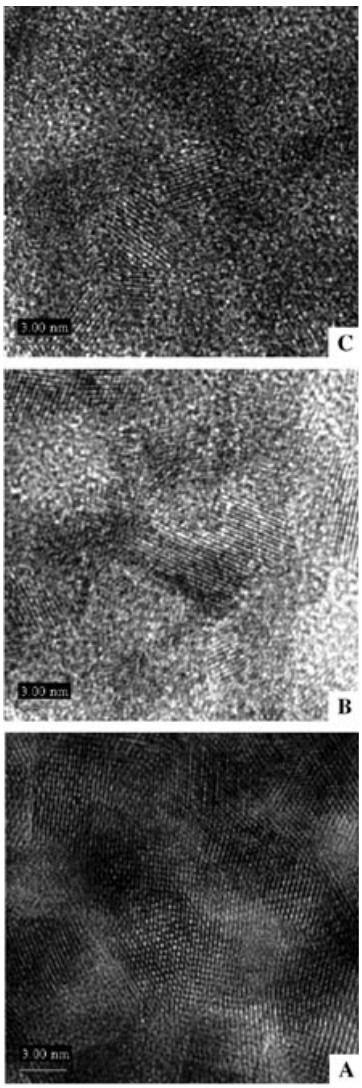

Figure 1. TEM images of JML-1 catalysts. Molar ratio of Zr/TrEOS/SiO_2 = 40:0.01:100 (a); 40:0.06:100 (b), and 40:0.11:100 (c). The bars represent 3 nm.

on these observations, a triethoxysilane amount of 0.06 mol % was selected in most of our experiments for a balanced consideration of both SZ nanocrystal size and surface coverage.

During the synthesis of JML-1, it is necessary to get a transparent mixture of the silica and zirconia solutions, that is, the two solutions should be mixed homogeneously at the nanometer scale. In the silica matrix, the addition of $HSi(OC_2H_5)_3$ promoted the gelation and condensation of oligosilicates to form a three-dimensional silica network as shown in Figure 2a. Following the solid-phase nucleation mechanism,[22–24] the nuclei of ZrO_2 colloids filled in the network grids were first squeezed from the inside of silica matrix during the calcination. With the "outward migration" of ZrO_2 nanoparticles under thermodynamic driving forces, the nuclei combined with SO_4^{2-} and grew into nanocrystals to form a typical core–shell structure with SZ nanocrystals anchored on/in the silica surface (Figure 2b).

The N_2 adsorption isotherm (Figure 3) suggests a micro–mesoporous structure of the JML sample with a Brunauer–Emmet–Teller (BET) surface area of about 280 $m^2 g^{-1}$; this is much larger than that (190 $m^2 g^{-1}$) of SZ and non-nanodispersed SZ/SiO_2 catalysts reported.[25] The single pore volume of JML-1_{40} is 0.44 $mL g^{-1}$, and the median pore diameter is 6.3 nm. Temperature-programmed desorption (TPD) of ammonia (Figure 4) showed that JML-1_{40} calcined both under N_2 atmosphere and in air that had high acid strength. The high-temperature TPD peaks of JML-1_{40}, assigned to ammonia desorbing from the acidic sites, are slightly lower than those reported for superacid sulfated zirconia.[26,27]

Surface photovoltage spectroscopy (SPS) in Figure 5 was used to determine the surface acidity of JML-1 by measuring the transition of electrons between the interface and the surface. The JML-1_{40} calcined at 550 °C exhibited two peaks at 596 and 677 nm, whereas the sample without calcination had only one peak at 330 nm. The peak at 330 nm is assigned to the band–band electron transition and those at 596 and 677 nm are attributed to the surface-related transitions. The observation of these surface-related transitions indicates the presence of positive charges on the surface of the calcined sample, suggesting that the acidity of JML-1 catalyst results from a large amount of SZ acidic sites on the silica surface.

The pyridine adsorption/desorption infrared spectra (Figure 6) of JML-1_{40} at various temperatures showed that, as the desorption temperature was increased, the intensity of the peak at 1449 cm^{-1} (Lewis acidic site) was almost unchanged, whereas that at 1545 cm^{-1} (Brønsted acidic site) decreased significantly. However, both of these bands still co-existed at 450 °C, and the intensity was about 50–60 % of that at room temperature. These results suggest that both Lewis and Brønsted acids coexist in JML-1.

The 1-butene conversion and product distribution obtained at 25 °C after 1 hour of alkylation reaction of isobu-

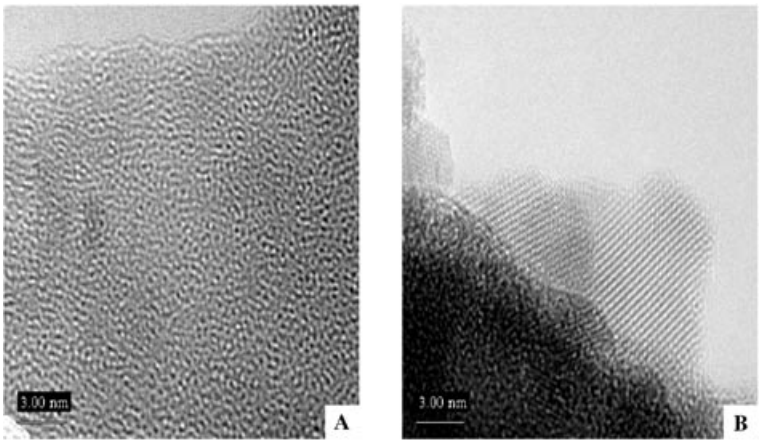

Figure 2. TEM images of materials prepared at A) Zr/TrEOS/Si = 0:0.06:100 and B) Zr/TrEOS/Si = 40:0.06:100 molar ratios. The bars represent 3 nm.

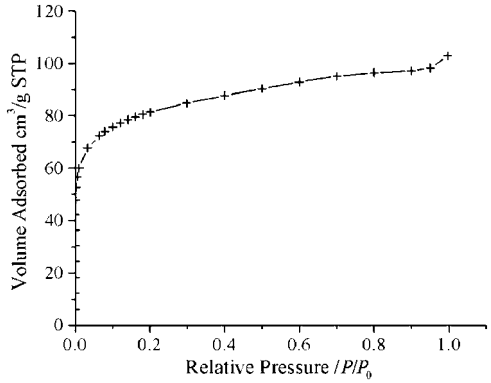

Figure 3. N_2 adsorption isotherm of JML-1_{50} (calcined at 550°C under N_2).

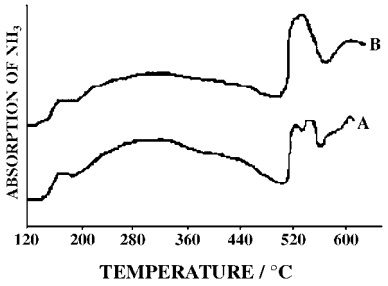

Figure 4. TPD curves of JML-1_{50} calcined at 550°C A) in air and B) in N_2.

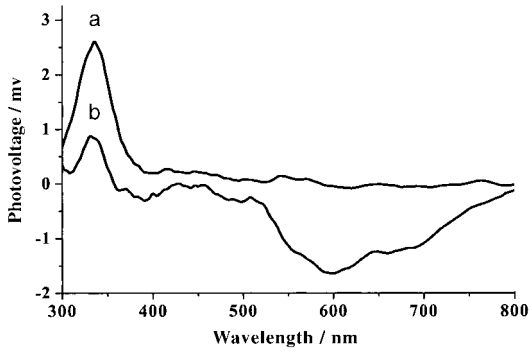

Figure 5. SPS of JML-1_{50} a) before and b) after being calcined at 550°C under N_2.

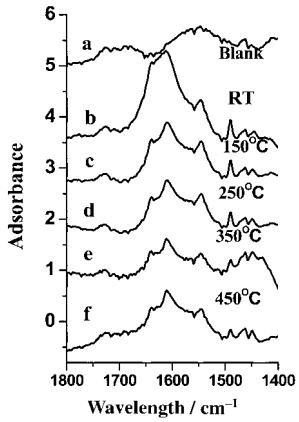

Figure 6. IR spectra of pyridine adsorbed/desorbed on JML-1_{40}. a) Adsorption at 450°C; desorption at b) room temperature; c) 150°C; d) 250°C; e) 350°C; f) 450°C.

tane on JML-1_{50} and zeolite Beta catalysts are summarized in Table 1. The conversion (97%) with JML-1_{50} catalyst is higher than that (86%) with zeolite Beta. The primary products with above catalysts are C_8 compounds (59.9% with JML-1_{50} and 62% with zeolite Beta). The C_8 products mainly consist of trimethylpentanes (TMPs), 58.7% for JML-1_{50} and 73% for zeolite Beta. The TMP/DMH (dimethylhexane) ratios are 13.5 for JLM-1_{50} and 4.1 for zeolite Beta, demonstrating that the selectivity of JML-1_{50} is higher than that of zeolite Beta. The yields of alkylate are 6.6 and 5.2 mL for JML-1_{50} and Beta zeolite, respectively. The weights of alkylate produced per weight of butene fed to the reactor are 1.13 and 0.95 for JML-1_{50} and zeolite Beta, respectively.

JML-1 exhibited a higher catalytic activity in many of catalytic reactions over a longer operation time than other catalysts. The alkylation reaction of isobutane with 1-butene (Figure 7) showed that JML-1_{50} (Zr/Si = 50:100 mol/mol) retained an activity of 95% after catalytic reaction for 20 h. Even after being regenerated five times, it kept its activity at over 90%. In a sharp contrast, the SZ and SZ/SiO_2 (Zr/Si = 50:100, mol/mol) showed very high activities only within the first 2 h of the reaction, and then lost their activity quickly; this is similar to the results of Corma's work.[23,24] For comparison, the initial activity of zeolite Beta and ZSM-5 were 88% and 60%, respectively, in the same alkylation reaction. For the condensation reaction of diethylene glycol to dioxane, JML-1_{40} gave a 92% yield of pure dioxane, while ZSM-5 only afforded 70% of yield within 1 h of reaction. Similarly, JML-1_{40} gave much higher yields than zeolite Y and ZSM-5 in the isomerization of *n*-pentane (Figure 8a) and in the cracking of isopropyl benzene (Figure 8b) at the same given reaction time. The high activity shown by the JML-1 catalytic system could be attributed to its unique core–shell structure and high dispersion of discrete SZ nanocrystals on the surface of silica matrix. This allows for the easy diffusion of the reactants and oxygen that leads to the

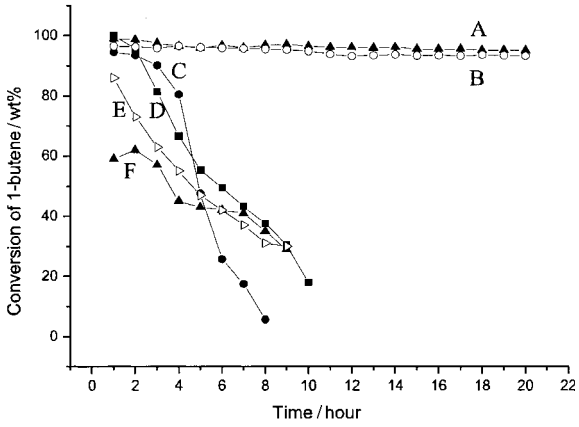

Figure 7. Catalytic conversion of 1-butene in the alkylation of isobutane with 1-butene (at a mole ratio of 12:1) versus reaction time for various catalysts (1 g each): A) JML-1_{50}; B) JML-1_{50} regenerated five times by calcination and sulfation; C) SZ); D) SZ/SiO_2 (Zr/Si = 50:100, mol/mol); E) zeolite Beta (SiO_2/Al_2O_3 = 40); F) zeolite ZSM-5 (SiO_2/Al_2O_3 = 40).

Table 1. The 1-butene conversion and product distribution after 1 h of alkylation reaction of isobutane on the as-prepared JML-1_{50} and zeolite Beta catalysts.

	Conversion of 1-butene[a]	Alkylate distribution[a]			Distribution of C_8[a]			TMP/DMH ratio
		C_5–C_7	C_8	C_9+	TMP[b]	DMH[c]	C_{other}	
JLM-1_{50}	97	14.4	59.9	25.7	58.7	4.34	39.2	13.5
Beta	86	29	62	9	73	18	9	4.1

[a] wt %. [a] Trimethylpentane. [b] Dimethylhexane.

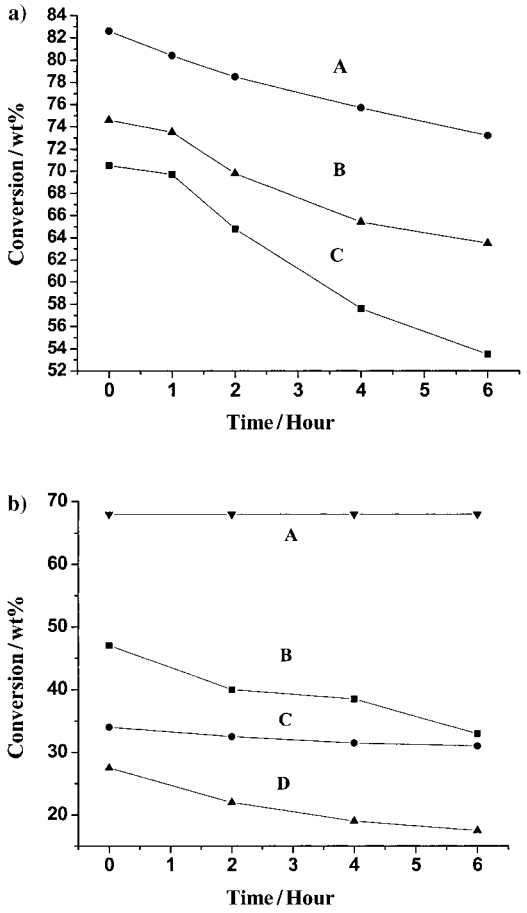

Figure 8. a) Isomerization of pentane over A) sulfated zirconia, B) JML-1_{40}, C) zeolite Y, and D) zeolite ZSM-5; b) Cracking of isopropyl benzene over A) JML-1_{40}; B) zeolite Y, and C) zeolite ZSM-5.

lowest carbon deposition and coke formation. However, in the pentane isomerization, conventional sulfated zirconia performed with higher activity than JML-1_{40} (Figure 8a). This is due to the lower surface sulfated zirconia density of JML-1_{40} relative to pure sulfated zirconia.

Due to the special structure, JML-1 prevents the SZ nanocrystals from self-agglomeration, and keeps its stability during the catalytic reaction over a long period of time, even after regeneration by calcination and sulfation many times. The JML-1 nanocatalyst system with high efficiency, long utilizing lifetime with good regeneratability, high catalytic activity and high stability over a long period of reaction time, as achieved successfully by this novel sol–gel process, would have a great potential for practical applications in solid catalytic reactions. The technique can be readily applied to the synthesis of other silica-supported metals or metal oxides, such as TiO_2/SiO_2, CuO/SiO_2, Pt/SiO_2, Au/SiO_2, and so forth, for various industrial catalytic reactions.

Acknowledgement

We thank Dr. B. Zhou, Prof. Da Z. Jiang, and Prof. T. H. Wu for valuable discussions. We thank Professors W. Y. Zhang and S. Lin for technical assistance. We are most grateful to the State Basic Research Project (G2000077507) and the National Natural Science Foundation of China for the financial support.

[1] B. Li, R. D. Gonazalez, *Ind. Eng. Chem. Res.* **1996**, *35*, 3141–3148.
[2] D. Farcasiu, J. Q. Li, *Catal. Rev.* **1996**, *38*, 329–412.
[3] D. Zalewski, S. Alerasool , P. Doolin, *Catal. Today* **1999**, *53*, 419–432.
[4] S. Bettina, T. Markus, K. C. Bettina, *Ind. Eng. Chem. Res.* **2001**, *40*, 2767–2772.
[5] P. H. Cuong, B. Christophe, D. Thierry, E. Babrielle, E. Claude, J. L. Marc, *Appl. Catal. A* **1999**, *180*, 385–397.
[6] Y. Y. Huang, B. Y. Zhao, Y. C. Xie, *Appl. Catal. A* **1998**, *171*, 65–73.
[7] T. Yamaguchi, T. Jin, T. Ishida, K. Tanabe, *Mater. Chem. Phys.* **1987**, *17*, 3; H. Althues, S. Kaskel, *Langmuir* **2002**, *18*, 7428–7435.
[8] T. Ishida, T. Yamaguchi, K. Tanabe, *Chem. Lett.* **1988**, 1869.
[9] M. S. Wong, H. C. Huang , J. Y. Ying, *Chem. Mater.* **2002**, *14*, 1961–1973.
[10] K. Tomishige, A. Okabe, K. Fujumoto, *Appl. Catal. A* **2000**, *194*, 383–393.
[11] J. R. Sohn, H. J. Jang, *J. Mol. Catal.* **1991**, *64*, 349–360.
[12] T. Lopez, J. Navarrete, R. Gomez, O. Novaro, F. Figueras, H. Armendariz, *Appl. Catal. A* **1995**, *125*, 217–232.
[13] C. Morterra, G. Cerrato, F. Pinna, *Appl. Catal. A* **1999**, *176*, 27–43.
[14] D. Farcasiu, J. Q. Li, S. Cameron, *Appl. Catal. A* **1998**, *175*, 1–9.
[15] M.-T. Tran, N. S. Gnep, G. Szabo, M. Guisnet, *Appl. Catal. A* **1998**, *171*, 207–217.
[16] P. Canton, R. Olindo, F. Pinna, G. Strukul, P. Riello, M. Meneghetti, G. Cerrato, C. Morterra, A. Benedetti, *Chem. Mater.* **2001**, *13*, 1634–1641.
[17] A. Corma, *Chem. Rev.* **1995**, *95*, 559–614.
[18] X. Song, A. Sayari, *Catal. Rev. Sci. Eng.* **1996**, *38*, 329.
[19] C. I. Odenbrand, S. Andersson, L. Andersson, J. Brandin, G. Busca, *J. Catal.* **1990**, *125*, 541–553.
[20] T. Makoto, *J. Mol. Catal.* **1994**, *94*, 85–96.
[21] H. J. M. Bosman, E. C. Kruissink, J. Vanderspoel, F. Vandenbrink, *J. Catal.* **1994**, *148*, 660–672.
[22] B. Q. Xu, T. Yamaguchi, K. Tanabe, *Appl. Catal.* **1991**, *75*, 75–86.
[23] T. Yamaguchi, T. Jin, T. Ishida, K. Tnabe, *Mater. Chem. Phys.* **1978**, *7*, 17.
[24] L. M. Kustov, V. B. Kazansky, F. Figueras, D. Tichit, *J. Catal.* **1994**, *150*, 143–149.
[25] Y. Parulescu, S. Coman, P. Grange, V. I. Parvulescu, *Appl. Catal. A* **1999**, *176*, 27–43.
[26] A. Corma, A. Martinez, C. Martinez, *J. Catal.* **1994**, *149*, 52–60.
[27] A. Corma, M. I. Juan-Rajadell, J. M. Lopez-Nieto, A. Martinez, C. Martinez, *Appl. Catal. A* **1994**, *111*, 175–189.

Received: March 24, 2004
Published online: August 10, 2004